The Warm-period Daily Precipitation Extremes Scaling with Temperature in Eastern China

Danqing Huang[1*], Jian Zhu[2], and Xiaowen Tang[3]

1 School of Atmospheric Sciences, Nanjing University, Nanjing 210023, China

2 College of Hydrology and Water Resources, Hohai University, Nanjing 210098, China

3 College of Atmospheric Sounding, Chengdu University of Information Technology, Chengdu 610225, China

Submitted to *Geophysical Research Letters*

Date: August 26, 2020

[*]Corresponding author:

Dr. Danqing Huang

School of Atmospheric Sciences

Nanjing University

Nanjing 210023

The People's Republic of China

E-mail: huangdq@nju.edu.cn

Abstract

Using station and reanalysis datasets, the application of C-C scaling in understanding the relation between precipitation extremes and temperature in eastern China has been examined. The results show that the C-C scaling could be used to understand the daily precipitation extreme intensity increase with T_m, as it is below ~25ºC. However, as T_m exceeds 25ºC, the daily precipitation extremes would decrease with T_m, particularly for South China. The change in the variation as T_m exceeds 25ºC may be attributed to the negative scaling of precipitation efficiency and vertical velocity with T_m. The sharp increase in the convective inhibition, decrease in the temperature advection, can partly explain the negative scaling of precipitation efficiency and T_m, vertical velocity and T_m as it exceeds 25ºC, respectively. Our results show physical image linking the precipitation extremes and temperature variation, which would likely help understanding the variations in precipitation extremes under a warmer future.

Key Points:

1, The relation between the precipitation extremes and temperature as it exceeds ~25ºC deviates from the C-C scaling, particularly in South China.

2, The conceptual model indicates that this deviation may be attributed to the negative scaling of precipitation efficiency/vertical velocity with temperature.

3, The increase in convective inhibition, decrease in temperature advection with temperature, can partly explain the negative scaling of precipitation efficiency, vertical velocity and temperature, respectively.

1. Introduction

The variation of precipitation extremes by anthropogenic climate change is of great concern for the society [*Min et al.*, 2011; *Zhang et al.*, 2013; *Drobinski et al.*, 2016; *Prein et al.*, 2017b; *Baker et al.*, 2018]. Although, the response of precipitation extremes to warming is one of the key uncertainties associated with climate change [*Hawkins and Sutton*, 2009; *Huang et al.*, 2013, 2018], it is generally agreed that the increasing warming could modify precipitation characteristics in terms of the amount, frequency and intensity [*Huang et al.*, 2019].

The association between precipitation extremes and temperature, termed as 'scaling', is theoretically linked to the Clausius–Clapeyron (C–C) relationship, which predicts roughly a 7% (C-C scaling) increase in the daily precipitation extremes associated with atmospheric warming [*Trenberth et al.*, 2003; *Pall et al.*, 2007; *Bui et al.*, 2019]. Generally, observations and simulations with climate models have reported a variety of scaling rates between daily precipitation extremes and temperature, including strong C-C scaling in Europe [*Trenberth et al.*, 2003; *Lenderink and Meijgaard*, 2008, 2010; *Berg et al.*, 2013; *Schroeer and Kirchengast*, 2018], but weak C-C scaling in North America [*Mishra et al.*, 2012; *Lepore et al.*, 2015] or even negative rates in the tropics [*O'Gorman*, 2012; *Drobinski et al.*, 2016; *Yin et al.*, 2018]. Thus, the rate of increase in the extreme daily precipitation intensity was not necessarily consistent with the C-C scaling. We should also notice that the relation is complicated as the temporal resolution of measurement of precipitation data changes (e.g., hourly or 5- minutes station data). As daily mean temperature is below ~25ºC, the rate of increase in hourly precipitation extremes is > 7% (even 14%, as super-C-C scaling) per warming degree [*Westra et al.*, 2014; *Prein et al.*, 2017b]. Besides of the positive relation between daily precipitation extremes and temperature, when

temperature exceeds ~25ºC, the intensity of precipitation extremes at different time-scales (daily, hourly, 5-minites) consistently begins to decrease [*Lenderink and Meijgaard*, 2010; *Utsumi et al.*, 2011; *Huang et al.*, 2017, 2019]. Thus, the different intensification rate of precipitation extremes in different regions and different temporal resolution of precipitation data demonstrates the complexity of the issue in application of the C-C scaling [e.g., *Zhang et al.*, 2017].

Eastern China is already very sensitive to climate change at short and long-time scales. Dominated by the Asian monsoon system [*Zhou et al.*, 2009], eastern China is vulnerable to precipitation extremes, which show significant regional discrepancy [*Zhai et al.*, 1999, 2005; *Wang et al.*, 2012; *Zhu et al.*, 2016]. Generally, precipitation extremes have frequently occurred over Yangtze River Basin [*Wang and Zhou*, 2005; *Zhai et al.*, 2005; *Fu et al.*, 2013] and South China [*Yao et al.*, 2008] and rarely occurred over Sichuan Basin [*Zhai et al.*, 2005]. The intensity of precipitation extremes are strong in South China, while northern part of China (north to 35°N) has been recently suffered from some destructive precipitation extremes [*Li et al.*, 2016; *Lyu et al.*, 2016]. Most previous studies on the precipitation extremes in China have focused on the definitions, tendency, typical large-scale circulations, projections, detection of human influence, etc [*Sun and Ao*, 2013; *Zhou et al.*, 2014; *Chen and Sun*, 2017]. However, less study has paid attention to theoretical explanation on the sensitivity of extreme rainfall to atmospheric temperature. Some studies have focused on some specific regions, as South China [*Sun et al.*, 2013], Anhui Province [*Huang et al.*, 2017]. Although the C-C scaling can explain the relation between daily precipitation extremes and temperature, they consistently show the deviation from the C-C scaling, particularly for different regions.

Many factors can contribute to departure from C-C scaling: temporal and spatial

averaging, choice of scaling temperature [*Bui et al.*, 2019], the precipitable water and vertical velocity [*Kunkel et al.*, 2020], precipitation efficiency [*Huang et al.*, 2019], dynamical conditions [*Drobinski et al.*, 2016], the precipitation types [*Berg et al.*, 2013], and etc.. Particularly for the negative scaling of daily precipitation extremes on temperature exceeding ~25 ºC, it may due to the decrease in relative humidity [*Barbero et al.*, 2018], duration of precipitation events [*Utsumi et al.*, 2011], intermittency of rainfall at higher temperature [*Schleiss*, 2018], and the negative scaling of precipitation efficiency and temperature [*Huang et al.*, 2019], etc. Since the examination of C-C scaling in the relationship between the extreme daily precipitation intensity and temperature across eastern China and the possible reasons are still uncertain, here, we aimed to answer the following two questions using both of synoptic observations and reanalysis datasets: 1) Is the precipitation extremes scaling with temperature in different sub-regions over eastern China following the C-C scaling? 2) If it remains deviate from the C-C scaling, how to understand the deviation?

2. Data and methods

2.1 Data

The datasets used in this study are:

(1) The daily precipitation and mean air temperature of 2420 quality-controlled stations (Fig. 1a) over China during the period of 1979-2014 provided by China Meteorological Administration (http://data.cma.cn/site/index.html). Particularly, we focused four sub-regions of eastern China (Fig.1a): Northeastern China (110º-135ºE, 43º-54ºN), North China (110º-122ºE, 33º-53ºN), Yangtze-Huaihe

River Basin (110º-122ºE, 28º-34ºN), South China (110º-122ºE, 20º-27ºN).

(2) The European Centre for the Medium-Range Weather Forecasts (ECMWF) interim reanalysis (~0.75º×~0.75º) (ERA-Interim, Dee et al. 2011). The ERA-Interim reanalysis data has a good performance in describing precipitation and circulations in East Asia [*Lin et al.*, 2014; *Huang et al.*, 2016; *Zhu et al.*, 2017] and it also has the ability to understand the C-C scaling of daily precipitation extremes and temperature [*Huang et al.*, 2019]. The daily variables of mean temperature, specific humidity, sea level pressure and precipitation on the period of 1979-2014 are used.

2.2 Methods

Precipitation efficiency (E) measures the percentage of moisture in the air converting into precipitation. It is calculated as dividing daily precipitation by daily total precipitable water vapor [*Tuller*, 1973].

Using both synoptic observations and the ERA-Interim reanalysis, the scaling of precipitation extremes with daily mean temperature has been analyzed, following the two-step analysis procedure in *Lenderink and Meijgaard* [2008]. First, we stratified the daily precipitation data based on daily mean temperature in bins of 2ºC width. Second, we calculated the 90-95% and 95-99% of the distribution in each bin of precipitation events. To avoid the effect of snow, only precipitation events with daily mean temperature above 5ºC are selected.

Following *Chen et al.* [2020], the convective inhibition (in J/kg) is calculated as,

$$\mathrm{CIN} = R_d \int_{P(LFC)}^{p(SFC)} (T_{vp} - T_{ve}) d\ln(p)$$

Where R_d is the gas constant of dry air, and p is the air pressure. Here,

147 T_{vp} *and* T_{ve}, the virtual temperature of the lifted parcel and the environment
148 respectively, are used to account for the effect of water vapor on air density [*Doswell*
149 *and Rasmussen*, 1994]. The definitions of CIN is widely recognized and consistent
150 with many previous studies [e.g. *Dai et al.*, 1999; *Riemann-Campe et al.*, 2009; *Prein*
151 *et al.*, 2017a].

152

153 # 3. Results

154 ## 3.1 Scaling of precipitation extremes with temperature

155 Figure 1 shows the dependency of different percentiles of daily precipitation
156 extremes on daily mean temperature (T_m) in eastern China by using synoptic
157 observations (middle panels). In eastern China, while T_m is below ~25ºC, daily
158 precipitation extremes increase with the increase of T_m, following the rate of the C-C
159 scaling (the grey dot lines), ~7%. However, precipitation extremes start to decrease
160 when T_m exceeds ~25ºC, particularly in YHRB and SC. This behavior is robust
161 throughout the domain for the extreme percentiles (90-95%, 95-99%). Actually, this is
162 also robust for the percentiles above 70% in eastern China [*Huang et al.*, 2019] and
163 the percentiles between 20%-80% in the French Mediterranean region [*Drobinski et*
164 *al.*, 2016]. In fact, temperature when the slope change is different for each regions.
165 There are ~21 ºC, 24 ºC, 25 ºC and 26 ºC for NEC, NC, YHRB and SC, respectively.
166 This may partly due to the climatology in different sub-regions. The ERA-Interim
167 reanalysis can also capture the relation between the daily precipitation extremes and
168 T_m in eastern China (right panels), which is also proved by some recent studies for
169 Europe and North America [e.g., *Lenderink et al.*, 2017; *Wang et al.*, 2017]. Thus, in
170 the eastern China, both of the synoptic observations and reanalysis datasets confirm
171 that the C-C scaling could indicate the daily precipitation extreme intensity increasing

with T_m below ~25ºC. On the contrast, as T_m exceeds 25ºC, the daily precipitation extremes would decrease with T_m. We should also notice the regional differences, mostly for the changing temperature and rate of the decreasing slope. This negative relation between precipitation extremes and T_m has deviated from the C-C scaling.

3.2 Understanding the scaling of precipitation extremes with temperature

In 1996, *Charles A. Doswell III et al.* [1996] has introduced a conceptual model of precipitation extremes,

$$P = Ewq \quad (1)$$

Where P is the precipitation intensity, E is the precipitation efficiency, w is the vertical velocity, q is the mixing ratio of the rising air. This means rising air should have a substantial water vapor content and a rapid ascent rate if a significant precipitation rate is to develop. Differentiating the conceptual model (1) with respect to a temperature T gives,

$$\frac{\partial P}{\partial T} = q \cdot w \cdot \frac{\partial E}{\partial T} + q \cdot E \cdot \frac{\partial w}{\partial T} + w \cdot E \cdot \frac{\partial q}{\partial T} \quad (2)$$

Changes in precipitation efficiency and vertical velocity with temperature could partly explain the departures from C-C scaling. Following *Emori and Brown* [2005], we choose vertical pressure velocity at 500hPa (W500) and total precipitable water vapor as w and q in equation (2), respectively. Thus, we individually focus on the $\frac{\partial E}{\partial T}$, $\frac{\partial w}{\partial T}$ and $\frac{\partial q}{\partial T}$, which is shown in Figure 2.

On the one hand, the dependency of different percentiles of daily precipitation efficiency and T_m (Fig. 2a-d) shows quite consistent results in that between W500 and T_m (Fig. 2e-h) in the four sub-regions. As T_m is below 25ºC, the precipitation efficiency slowly increases and the W500 is quite stable as T_m increases. Similarly,

196 the precipitation efficiency and W500 decreases as T_m exceeds 25ºC. Thus, the
197 out-of-phase relationship between precipitation extremes and T_m may be partly
198 explained by that between precipitation efficiency and T_m, and vertical velocity and
199 T_m.

200 On the other hand, as expected, governed by the C-C equation, the atmospheric
201 moisture increases with T_m following the C-C scaling (Fig.2i-l). In fact, we can notice
202 that the relation still reverses like that between precipitation extremes and T_m, but the
203 turning point is ~27 ºC of T_m. The reversal in the scaling may be due to moisture
204 limitations at higher temperatures as seen in previous studies [*Bao et al.*, 2017;
205 *Barbero et al.*, 2018]. Thus, we may infer that the C-C scaling can largely explain the
206 relation between precipitation extremes and T_m below 25 ºC. As T_m exceeds 25ºC, the
207 reverse relation may be partly due to the negative relation between the precipitation
208 efficiency (vertical motion) and T_m.

209 With respect to $\frac{\partial E}{\partial T}$ (Fig.2a-d) and $\frac{\partial w}{\partial T}$ (Fig.2e-h), the possible factors have
210 been further investigated. In fact, the precipitation efficiency has significant negative
211 correlated with the convective inhibition (CIN) [*Market et al.*, 2003] . This significant
212 negative relationship between precipitation efficiency and CIN is also confirmed in
213 eastern China, particularly as the CIN exceeds 50 J/kg (Fig.3a) and also found in
214 sub-regions (Figure not shown). The relation between the CIN and T_m in four
215 sub-regions has been further examined (Fig.3c, e, g, i). These results were categorized
216 into two major groups. In the northern part of China (NEC, Fig.3c and NC, Fig.3e),
217 the CIN increases as T_m increases for NEC and NC. On the contrast, the relation
218 between T_m and CIN are complicated in the southern part of China (YHRB and SC).
219 The CIN has increased as the T_m increases, except the T_m is between 25ºC-27ºC.

Particularly, in SC, as T_m is higher than 27ºC, CIN significantly increases as T_m rises. Thus, the significant increases in CIN in the high T_m would favor the decrease in the precipitation efficiency. In fact, this relationship is more obvious in South China than other regions. As well, uncertainties also exists in southern part of China as the T_m is between 25ºC-27ºC. These would remind us the importance of regional difference.

The positive correlation between the vertical velocity and temperature advection ($-\vec{V} \cdot \nabla T$) has been established by the quasi-geostrophic omega equation [*Jonathan E Martin*, 2006], suggesting that the warm advection would favor the ascend motion, and vice versa. This positive relation is well established in eastern China (Fig.3b) and also found in sub-regions (Figure not shown). Similarly, we further investigated the relation between the temperature advection and T_m in the four sub-regions (Fig.3d, f, h, j). Generally, as T_m is below 20ºC, the temperature advection shows not much tendency with the increases of the T_m, while as T_m is above 20 ºC, the slope is negative, indicating the temperature advection decreases as the T_m increases. There are also regional differences, suggesting more significant negative slope in YHRB (Fig.3h) and South China (Fig.3j), compared to other regions. Due to the positive relation between the vertical velocity and temperature advection, this negative slope between the temperature advection and T_m would contribute to that between the vertical velocity and T_m.

4. Conclusion and discussion

In eastern China, the C-C scaling could predict the daily precipitation extreme intensity increase with T_m, as the T_m is below 25ºC. However, as T_m exceeds 25ºC, the daily precipitation extremes would decrease with T_m, particularly for daily

precipitation extremes in South China. This negative relation between the precipitation extremes and temperature deviates from the C-C scaling.

Traced to the conceptual model of precipitation extremes, besides of the water vapor, the vertical velocity, precipitation efficiency scaling with the temperature may result in the deviation as T_m exceeds 25ºC. In fact, the water vapor, vertical velocity, precipitation efficiency consistently increase as the T_m increases. Therefore, the C-C scaling can largely explain the relation between precipitation extremes and T_m below 25 ºC. As T_m exceeds 25ºC, precipitation efficiency and vertical velocity significantly decrease with temperature rising, which can contribute to the departures from C-C scaling. Additionally, as T_m exceeds 25ºC, the sharp increase in CIN, decrease in the temperature advection with T_m may result in the negative relation between the precipitation efficiency and T_m, the vertical velocity and T_m, respectively.

Several questions still remain and need further analyses. First, the relative contributions of the vertical velocity and precipitation efficiency to the deviation should be quantitative distinguished. Second, we have found obvious regional distinctions (northern part and southern part of eastern China), which may due to the large-scale circulations, different kinds of precipitation extremes, dynamical conditions and etc. Third, we have attempted the similar analyses on the sub-daily datasets. However, our results show that the hourly precipitation extremes over the eastern China do not seem to exhibit super C-C scaling, unlike what was found in other observational studies (Figure not shown). These possible reasons should also be further investigated. Considering these would likely help us to understand the variations in different time-scale precipitation extremes under a warmer future.

Acknowledgements This study is sponsored by the National Key Research and

Development Program of China (Grant No. 2016YFA0600701) and the Jiangsu Collaborative Innovation Center for Climate Change. All datasets used herein are in the public domains and citations are provided within the text, including (1) The daily quality-controlled stations over China (available at http://data.cma.cn/site/index.html); (2) The ERA-Interim datasets (available at https://www.ecmwf.int/en/forecasts/datasets/reanalysis-datasets/era-interim)

References:

Baker, H. S., R. J. Millar, D. J. Karoly, U. Beyerle, P. Benoit, D. Mitchell, H. Shiogama, S. Sparrow, T. Woollings, and M. R. Allen (2018), Higher CO_2 concentrations increase extreme event risk in a 1.5◦C world, *Nat. Clim. Chang.*, 267–283, doi:10.1038/s41558-018-0190-1.

Bao, J., S. C. Sherwood, L. V. Alexander, and J. P. Evans (2017), Future increases in extreme precipitation exceed observed scaling rates, *Nat. Clim. Chang.*, *7*(2), 128–132, doi:10.1038/nclimate3201.

Barbero, R., S. Westra, G. Lenderink, and H. J. Fowler (2018), Temperature-extreme precipitation scaling: a two-way causality?, *Int. J. Climatol.*, *38*, 1274–1279, doi:10.1002/joc.5370.

Berg, P., C. Moseley, and J. O. Haerter (2013), Strong increase in convective precipitation in response to higher temperatures, *Nat. Geosci.*, *6*(3), 181–185, doi:10.1038/ngeo1731.

Bui, A., F. Johnson, and C. Wasko (2019), The relationship of atmospheric air temperature and dew point temperature to extreme rainfall The relationship of atmospheric air temperature and dew point temperature to extreme rainfall, *Environ. Res. Lett.*, *14*, 074025.

Charles A. Doswell III, H. E. Brooks, and R. A. Maddox (1996), Flash flood forecasting: An ingredients-based methodology, *Weather Forecast.*, *11*, 560–581.

Chen, H., and J. Sun (2017), Contribution of human influence to increased daily precipitation extremes over China, *Geophys. Res. Lett.*, *44*(5), 2436–2444, doi:10.1002/2016GL072439.

Chen, J., A. Dai, Y. Zhang, and K. L. Rasmussen (2020), Changes in convective available potential energy and convective inhibition under global warming, *J. Clim.*, *33*(6), 2025–2050, doi:10.1175/JCLI-D-19-0461.1.

Dai, A., F. Giorgi, and K. E. Trenberth (1999), Observed and model-simulated diurnal cycles of precipitation over the contiguous United States, *J. Geophys. Res. Atmos.*, *104*(D6), 6377–6402, doi:10.1029/98JD02720.

Dee, D. P. et al. (2011), The ERA-Interim reanalysis: configuration and performance of the data assimilation system, *Q. J. R. Meteorol. Soc.*, *137*, 553–597, doi:10.1002/qj.828.

Doswell, C. A., and E. N. Rasmussen (1994), The effect of neglecting the virtual temperature correction on CAPE calculations, *Weather Forecast.*, *9*(4), 625–629, doi:10.1175/1520-0434.

Drobinski, P., B. Alonzo, S. Bastin, N. Da Silva, and C. Muller (2016), Scaling of precipitation extremes with temperature in the French Mediterranean region: What explains the hook shape?, *J. Geophys. Res.*, *121*(7), 3100–3119, doi:10.1002/2015JD023497.

Emori, S., and S. J. Brown (2005), Dynamic and thermodynamic changes in mean and extreme precipitation under changed climate, *Geophys. Res. Lett.*, *32*(17), 1–5, doi:10.1029/2005GL023272.

Fu, G., J. Yu, X. Yu, R. Ouyang, Y. Zhang, P. Wang, W. Liu, and L. Min (2013), Temporal variation of extreme rainfall events in China, 1961–2009, *J. Hydrol.*, *487*, 48–59, doi:10.1016/j.jhydrol.2013.02.021.

Hawkins, E., and R. Sutton (2009), The Potential to Narrow Uncertainty in Regional Climate Predictions, *Bull. Am. Meteorol. Soc.*, *90*(8), 1095–1107, doi:10.1175/2009BAMS2607.1.

Huang, D., J. Zhu, Y. Zhang, and A. Huang (2013), Uncertainties on the simulated summer precipitation over Eastern China from the CMIP5 models, *J. Geophys. Res. Atmos.*, *118*, 9035–9047, doi:10.1002/jgrd.50695.

Huang, D., J. Zhu, Y. Zhang, Y. Huang, and X. Kuang (2016), Assessment of summer monsoon precipitation derived from five reanalysis datasets over East Asia, *Q. J. R. Meteorol. Soc.*, *142*, 108–119, doi:10.1002/qj.2634.

Huang, D., P. Yan, G. Liu, and J. Zhu (2017), Relationship between precipitation extremes with temperature in the warm season in Anhui Province, *Clim. Environ. Res. (in Chinese)*, *22*(5), 623–632.

Huang, D., P. Yan, J. Zhu, Y. Zhang, X. Kuang, and J. Cheng (2018), Uncertainty of global summer precipitation in the CMIP5 models: a comparison between high-resolution and low-resolution models, *Theor. Appl. Climatol.*, *132*(1–2), 55–69, doi:10.1007/s00704-017-2078-9.

Huang, D., P. Yan, X. Xiao, J. Zhu, X. Tang, and A. Huang (2019), The tri-pole relation among daily mean temperature , atmospheric moisture and precipitation intensity over China, *Glob. Planet. Change*, *179*, 1–9, doi:10.1016/j.gloplacha.2019.04.016.

Kunkel, K. E., S. E. Stevens, L. E. Stevens, and T. R. Karl (2020), Observed Climatological Relationships of Extreme Daily Precipitation Events with Precipitable Water and Vertical Velocity in the Contiguous United States, *Geophys. Res. Lett.*, *47*, doi:10.1029/2019GL086721.

Lenderink, G., and E. van Meijgaard (2010), Linking increases in hourly precipitation extremes to atmospheric temperature and moisture changes, *Environ. Res. Lett.*, *5*, 025208, doi:10.1088/1748-9326/5/2/025208.

Lenderink, G., and E. Van Meijgaard (2008), Increase in hourly precipitation extremes beyond expections from temperature changes, *Nature*, *1*, 511–514.

Lenderink, G., R. Barbero, J. M. Loriaux, and H. J. Fowler (2017), Super Clausius-Clapeyron scaling of extreme hourly convective precipitation and its relation to large-scale atmospheric conditions, *J. Clim.*, 6037–6052, doi:10.1175/JCLI-D-16-0808.1.

Lepore, C., D. Veneziano, and A. Molini (2015), Temperature and CAPE Dependence of Rainfall Extremes in the Eastern United States, *Geophys. Res. Lett.*, doi:10.1002/2014GL062247.

Li, H., J. Gao, Y. Zhang, X. Bai, P. Sun, and Y. Zhang (2016), Analysis of Yanan Extreme Rainfall Characterstics and Impacts of Erosion Disasters on Terraces, *J. Soil Water Conserv. (in Chinese)*, *30*(6), 79–84.

Lin, R., T. Zhou, and Y. Qian (2014), Evaluation of Global Monsoon Precipitation Changes based on Five Reanalysis Datasets, *J. Clim.*, *27*(3), 1271–1289, doi:10.1175/JCLI-D-13-00215.1.

Lyu, M., L. Sheng, Z. Zhang, and L. Zhang (2016), Distribution and accumulation of soil carbon in temperate wetland, northeast China, *Chinese Geogr. Sci.*, *26*(3), 295–303, doi:10.1007/s11769-016-0809-y.

Market, P., S. Allen, R. Scofield, R. Kuligowski, and A. Gruber (2003), Precipitation efficiency of warm season midwestern mesoscale convective systems, *Weather Forecast.*, *18*, 1273–1285.

Min, S.-K., X. Zhang, F. W. Zwiers, and G. C. Hegerl (2011), Human contribution to more-intense precipitation extremes, *Nature*, *470*(7334), 378–81, doi:10.1038/nature09763.

Mishra, V., J. M. Wallace, and D. P. Lettenmaier (2012), Relationship between hourly extreme precipitation and local air temperature in the United States, *Geophys. Res. Lett.*, *39*(16), doi:10.1029/2012GL052790.

O'Gorman, P. a. (2012), Sensitivity of tropical precipitation extremes to climate change, *Nat. Geosci.*, *5*(10), 697–700, doi:10.1038/ngeo1568.

Pall, P., M. Allen, and D. Stone (2007), Testing the Clausius–Clapeyron constraint on changes in extreme precipitation under CO_2 warming, *Clim. Dyn.*, *28*, 351–363, doi:10.1007/s00382-006-0180-2.

Prein, A. F., C. Liu, K. Ikeda, S. B. Trier, R. M. Rasmussen, G. J. Holland, and M. P. Clark (2017a), Increased rainfall volume from future convective storms in the US, *Nat. Clim. Chang.*, *7*(12), 880–884, doi:10.1038/s41558-017-0007-7.

Prein, A. F., R. M. Rasmussen, K. Ikeda, C. Liu, M. P. Clark, and G. J. Holland (2017b), The future intensification of hourly precipitation extremes, *Nat. Clim. Chang.*, *7*(1), 48–52.

Riemann-Campe, K., K. Fraedrich, and F. Lunkeit (2009), Global climatology of Convective Available Potential Energy (CAPE) and Convective Inhibition (CIN) in ERA-40 reanalysis, *Atmos. Res.*, *93*(1–3), 534–545, doi:10.1016/j.atmosres.2008.09.037.

Schleiss, M. (2018), How intermittency affects the rate at which rainfall extremes respond to changes in temperature, *Earth Syst. Dyn.*, *9*, 955–968, doi:doi.org/10.5194/esd-9-955-2018.

Schroeer, K., and G. Kirchengast (2018), Sensitivity of extreme precipitation to temperature: the variability of scaling factors from a regional to local perspective, *Clim. Dyn.*, *50*(11–12), 3981–3994, doi:10.1007/s00382-017-3857-9.

Sun, J., and J. Ao (2013), Changes in precipitation and extreme precipitation in a warming environment in China, *Chinese Sci. Bull.*, *58*(12), 1395–1401, doi:10.1007/s11434-012-5542-z.

Sun, W., J. Li, and R. Yu (2013), An Analysis on Relation Between Warm Season Precipitation Extremes and Surface Air Temperature in South China, *Progressus Inquistitiones Mutat. Clim. (in Chinese)*, *9*(2), 96–101, doi:10.3969/j.issn.1673-1719.2013.02.003.

Trenberth, K. E., A. Dai, R. R. M., and P. D. B. (2003), the changing character of precipitation.pdf, *Bull. Am. Meteorol. Soc.*, 1205–1217.

Tuller, S. E. (1973), Seasonal and annual precipitation efficiency in Canada,

Atmosphere (Basel)., 52–66, doi:10.1080/00046973.1973.9648348.
Utsumi, N., S. Seto, S. Kanae, E. E. Maeda, and T. Oki (2011), Does higher surface temperature intensify extreme precipitation?, *Geophys. Res. Lett.*, *38*(16), doi:10.1029/2011GL048426.
Wang, G., D. Wang, K. E. Trenberth, A. Erfanian, M. Yu, M. G. Bosilovich, and D. T. Parr (2017), The peak structure and future changes of the relationships between extreme precipitation and temperature, *Nat. Clim. Chang.*, *7*, doi:10.1038/nclimate3239.
Wang, H., J. Sun, H. Chen, Y. li Zhu, Y. Zhang, D. Jiang, X. Lang, K. Fan, E. Yu, and S. Yang (2012), Extreme climate in China: Facts, simulation and projection, *Meteorol. Zeitschrift*, *21*(3), 279–304, doi:10.1127/0941-2948/2012/0330.
Wang, Y., and L. Zhou (2005), Observed trends in extreme precipitation events in China during 1961-2001 and the associated changes in large-scale circulation, *Geophys. Res. Lett.*, *32*(9), 1–4, doi:10.1029/2005GL022574.
Westra, S., H. J. Fowler, J. P. Evans, L. V Alexander, P. Berg, F. Johnson, E. J. Kendon, G. Lenderink, and N. M. Roberts (2014), Future changes to the intensity and frequency of short-duration extreme rainfall, *Rev. Geophys.*, *52*, 522–555, doi:10.1002/2014RG000464.
Yao, C., S. Yang, W. Qian, Z. Lin, and M. Wen (2008), Regional summer precipitation events in Asia and their changes in the past decades, *J. Geophys. Res.*, *113*(D17), D17107, doi:10.1029/2007JD009603.
Yin, J., G. Pierre, S. Zhou, S. C. Sullivan, R. Wang, Y. Zhang, and S. Guo (2018), large increase in global strom runoff extremes driven by climate and anthropogenic changes, *Nat. Commun.*, doi:10.1038/s41467-018-06765-2.
Zhai, P., A. Sun, F. Ren, X. Liu, B. Gao, and Q. Zhang (1999), Changes of climate extremes in China, *Clim. Change*, *42*, 203–218, doi:10.1023/A:1005428602279.
Zhai, P., X. Zhang, H. Wan, and X. Pan (2005), Trends in Total Precipitation and Frequency of Daily Precipitation Extremes over China, *J. Clim.*, *18*, 1096–1108.
Zhang, X., H. Wan, F. W. Zwiers, G. C. Hegerl, and S.-K. Min (2013), Attributing intensification of precipitation extremes to human influence, *Geophys. Res. Lett.*, *40*(19), 5252–5257, doi:10.1002/grl.51010.
Zhang, X., F. W. Zwiers, G. Li, H. Wan, and A. J. Cannon (2017), Complexity in estimating past and future extreme short-duration rainfall, *Nat. Geosci.*, *10*(4), 255–259, doi:10.1038/ngeo2911.
Zhou, B., Q. Han Wen, Y. Xu, L. Song, and X. Zhang (2014), Projected Changes in Temperature and Precipitation Extremes in China by the CMIP5 Multi-model Ensembles, *J. Clim.*, *27*, 6591–6611, doi:10.1175/JCLI-D-13-00761.1.
Zhou, T., D. Gong, J. Li, and B. Li (2009), Detecting and understanding the multi-decadal variability of the East Asian Summer Monsoon – Recent progress and state of affairs, *Meteorol. Zeitschrift*, *18*(4), 455–467, doi:10.1127/0941-2948/2009/0396.
Zhu, J., D. Huang, Y. Dai, and X. Chen (2016), Recent heterogeneous warming and the associated summer precipitation over eastern China, *Theor. Appl. Climatol.*, *123*, 619–627, doi:10.1007/s00704-015-1380-7.
Zhu, J., D. Huang, P. Yan, Y. Huang, and X. Kuang (2017), Can reanalysis datasets describe the persistent temperature and precipitation extremes over China?, *Theor. Appl. Climatol.*, *130*(1–2), 655–671, doi:10.1007/s00704-016-1912-9.
Jonathan, E Martin, 2006. Mid-latitude atmospheric dynamics: A first course, Wiley, PP336.

457

458

459

Figures:

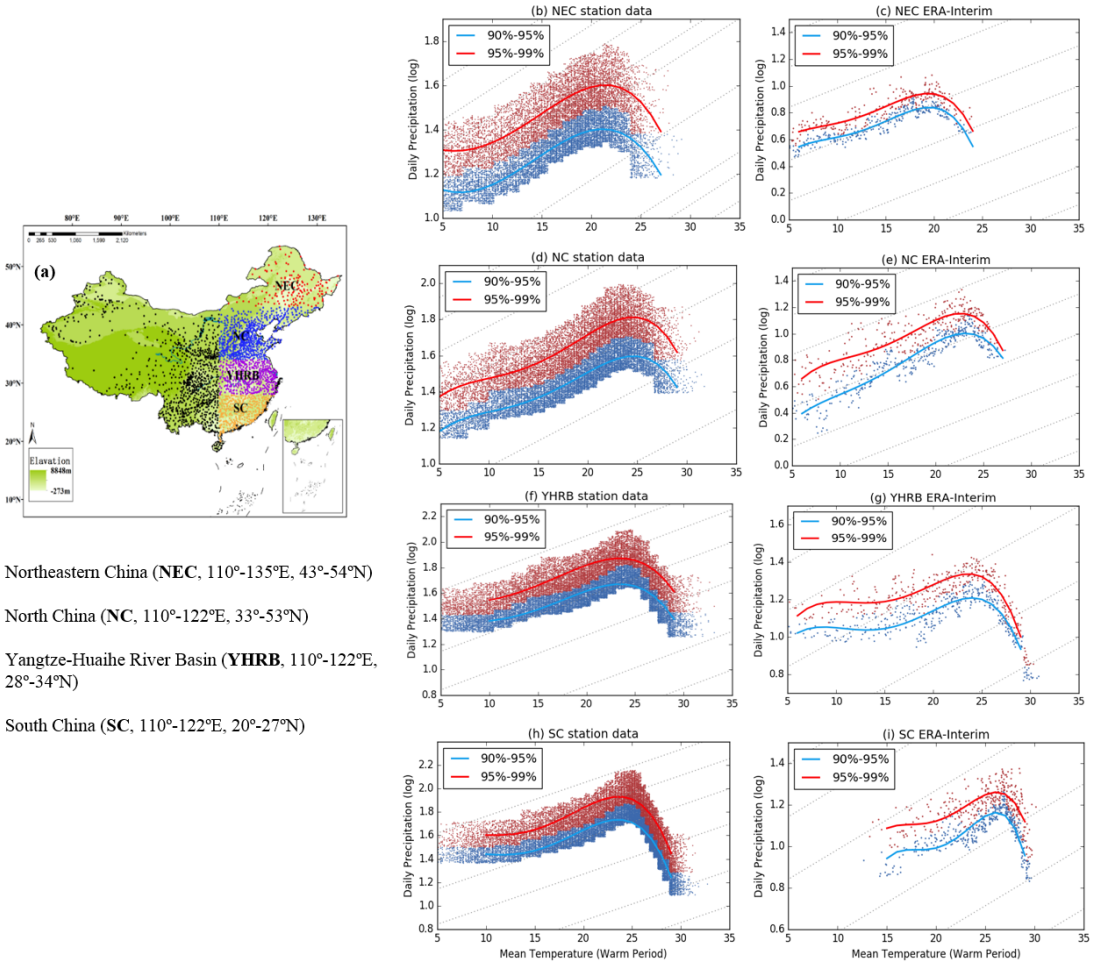

Figure 1 The distribution of the 2420 stations used in this study (a), and dependency of different percentiles of daily precipitation extremes on daily mean temperature in Northeastern China (NEC, b, c), North China (NC, d, e), Yangtze-Huaihe River Basin (YHRB, f, g) and South China (SC, h, i) from station data (middle panel) and ERA-Interim reanalysis datasets (right panel). The red, blue, purple and orange dots are for NEC, NC, YHRB and SC, respectively. Four sub-regions over eastern China: Northeastern China (NEC, 110°-135°E, 43°-54°N), North China (NC, 110°-122°E, 33°-53°N), Yangtze-Huaihe River Basin (YHRB,110°-122°E, 28°-34°N), South China (SC, 110°-122°E, 20°-27°N). Scatter points in (b-i) are computed from certain percentiles in each temperature bin. Solid curves are computed by the 4th degree exponential polynomial-fitting of precipitations. Colorful scatters and lines are for the different percentiles. Note the logarithmic Y-axis. Each dot in (middle panel) and (left panel) means the logarithmic daily precipitation for a certain station and a certain year in each sub-regions and sub-regional mean for a certain year from ERA-Interim reanalysis datasets, respectively.

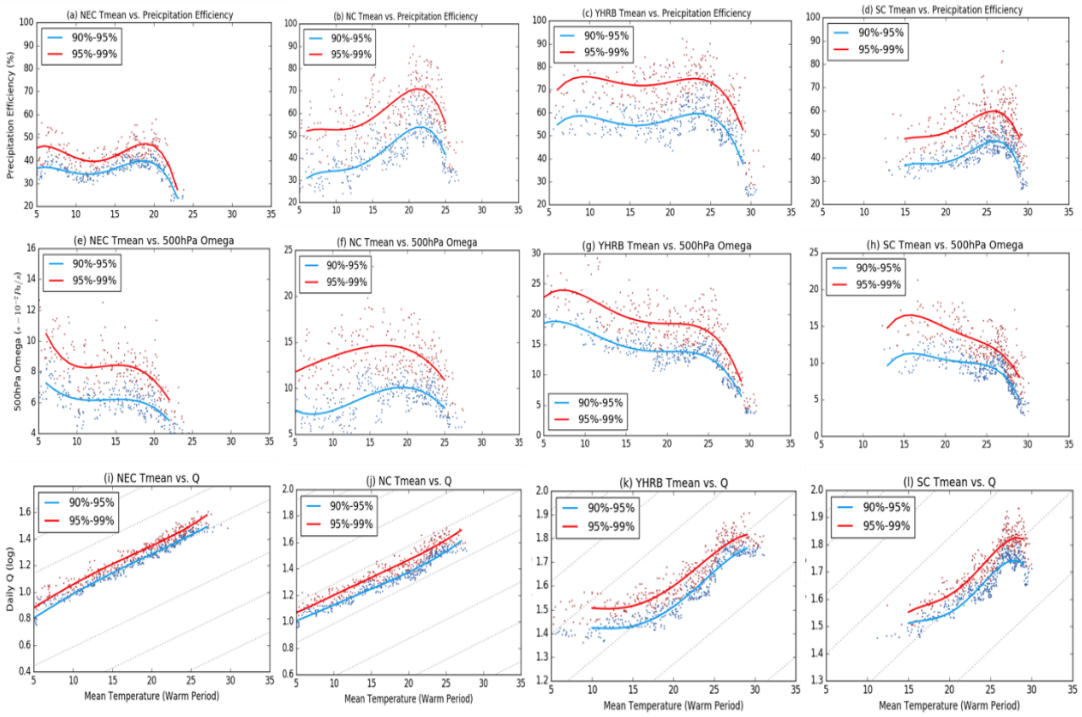

Figure 2 Dependency of different percentiles of daily precipitation efficiency (a-d, unit :%), vertical pressure velocity at 500hPa (e-h, unit: $(-1)*10^{-2}$ Pa/s) and the vertical integrated moisture transport from 1000 to 300hPa (i-l, short for Q) on daily mean temperature in NEC (first panel), NC (second panel), YHRB (third panel) and SC (forth panels) based on ERA-Interim reanalysis datasets. Solid curves are computed by the 4th degree exponential polynomial-fitting of precipitation efficiency, W and Q. Colorful scatters and lines are for the different percentiles. Note the logarithmic Y-axis in (i-l). Each dot in Figure 2 means the sub-regional mean value for a certain year from ERA-Interim reanalysis datasets.

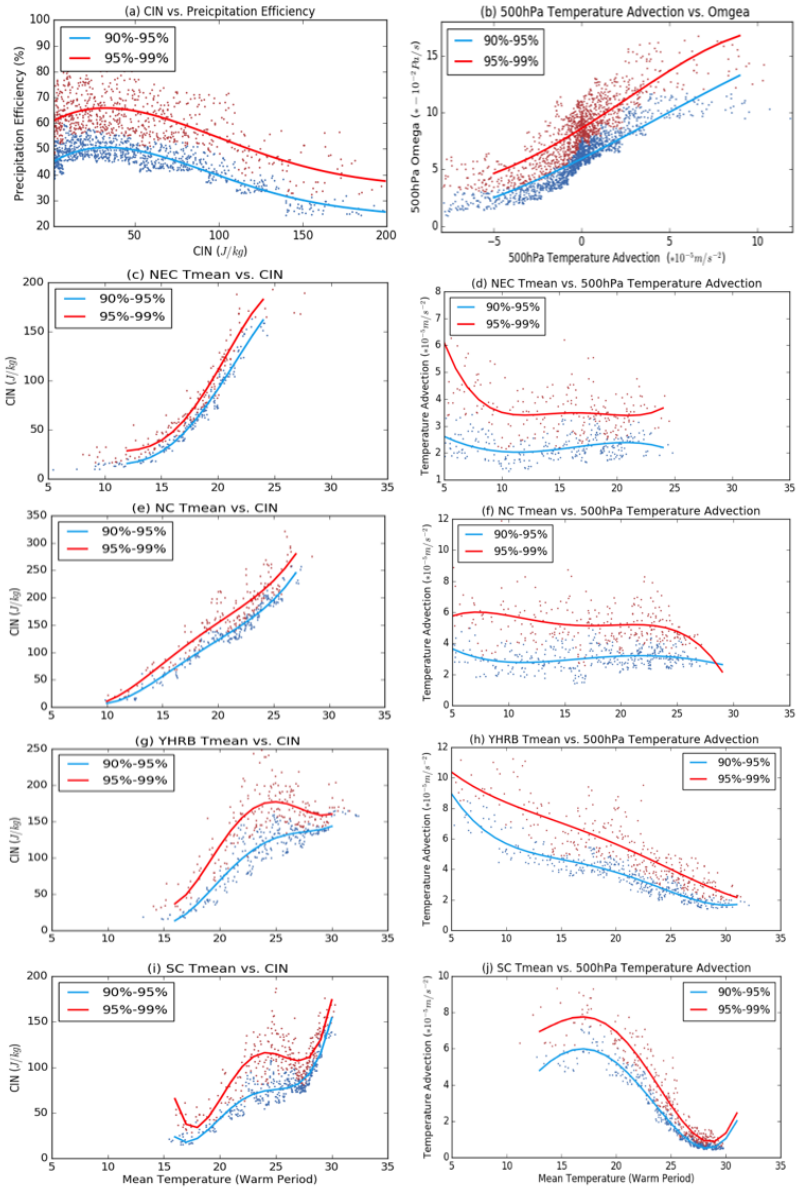

Figure 3 Dependency of different percentiles of daily precipitation efficiency (unit: %) on convective inhibition (a, CIN, unit: J/kg) and daily vertical pressure velocity at 500hPa (unit: (-1)*10^{-2} Pa/s) on temperature advection at 500hPa (b, unit: 10^{-5} m/s^{-2}) in eastern China, and the dependency of different percentiles of daily CIN (c, e, g, I, unit: J/kg) and daily temperature advection at 500 hPa (d, f, h, j, unit: 10^{-5} m/s^{-2}) on daily mean temperature in NEC (c, d), NC (e, f), YHRB (g, h) and SC (i, j). Solid curves are computed by the 4th degree exponential polynomial-fitting. Each dot in Figure 3 means the sub-regional mean value for a certain year from ERA-Interim reanalysis datasets.